DOI: 10.1002/chem.200902233

The Role of Solvent on the Mechanism of Proton Transfer to Hydride Complexes: The Case of the $[W_3PdS_4H_3(dmpe)_3(CO)]^+$ Cubane Cluster

Andrés G. Algarra,[a] Manuel G. Basallote,*[a] Marta Feliz,[b] M. Jesús Fernández-Trujillo,[a] Rosa Llusar,*[b] and Vicent S. Safont*[b]

Abstract: The kinetics of reaction of the $[W_3PdS_4H_3(dmpe)_3(CO)]^+$ hydride cluster ($\mathbf{1}^+$) with HCl has been measured in dichloromethane, and a second-order dependence with respect to the acid is found for the initial step. In the presence of added BF_4^- the second-order dependence is maintained, but there is a deceleration that becomes more evident as the acid concentration increases. DFT calculations indicate that these results can be rationalized on the basis of the mechanism previously proposed for the same reaction of the closely related $[W_3S_4H_3(dmpe)_3]^+$ cluster, which involves parallel first- and second-order pathways in which the coordinated hydride interacts with one and two acid molecules, and ion pairing to BF_4^- hinders formation of dihydrogen bonded adducts able to evolve to the products of proton transfer. Additional DFT calculations are reported to understand the behavior of the cluster in neat acetonitrile and acetonitrile–water mixtures. The interaction of the HCl molecule with CH_3CN is stronger than the W–H···HCl dihydrogen bond and so the reaction pathways operating in dichloromethane become inefficient, in agreement with the lack of reaction between $\mathbf{1}^+$ and HCl in neat acetonitrile. However, the attacking species in acetonitrile–water mixtures is the solvated proton, and DFT calculations indicate that the reaction can then go through pathways involving solvent attack to the W centers, while still maintaining the coordinated hydride, which is made possible by the capability of the cluster to undergo structural changes in its core.

Keywords: cluster compounds · density functional calculations · palladium · tungsten · kinetics · sulfides

Introduction

Protonation of transition-metal hydrides plays an important role in the study of catalytic ionic hydrogenation and reduction of H^+ to H_2, as well as for understanding the mechanism of biological systems as hydrogenases.[1–3] Many studies carried out during the last decade focused on the proton transfer mechanism between transition-metal hydrides and acids to give dihydrogen complexes.[4,5] Therefore, it has been shown that protonation of a transition-metal hydride is a formally simple process between a proton donor and a proton acceptor with several potential basic centers: the hydride, the metal and a basic ligand X.[6] Most of the information available to date indicates that attack occurs preferentially at the coordinated hydride and leads to formation of a dihydrogen complex [Eq. (1)], which can be stable or release H_2 in a subsequent step. The reaction steps and the position of the equilibrium of the proton-transfer reaction represented in Equation (1) depends on the relative acidity and basicity of interacting molecules and on the interaction with counterions,[7,8] or the solvent.[9] Theoretical and experimental investigations support the surrounding medium influence on the potential energy surface (PES) of the reaction mechanism.[6]

$$[L_nM{-}H] + HX \rightleftharpoons [L_nM(H_2)]^+ + X^- \rightleftharpoons [L_nM]^+ + H_2 + X^- \quad (1)$$

Processes like that in Equation (1) for cluster hydrides with $\{W_3(\mu_3\text{-}Q)(\mu\text{-}Q)_3\}$ (Q = S, Se) and $\{W_3Pd(\mu\text{-}S)_4\}$ core

[a] A. G. Algarra, Dr. M. G. Basallote, Dr. M. J. Fernández-Trujillo
Departmento de Ciencia de los Materiales e
Ingeniería Metalúrgica y Química Inorgánica
Facultad de Ciencias, Universidad de Cádiz
Campus Univ. Rio San Pedro. Puerto Real, 11510 Cádiz (Spain)
Fax: (+34) 956-016-288
E-mail: manuel.basallote@uca.es

[b] Dr. M. Feliz, Dr. R. Llusar, Dr. V. S. Safont
Department de Químíca Físca i Analítica
Universitat Jaume I, Campus de Riu Sec
Avda. Sos Baynat s/n. 12071, Castelló (Spain)
Fax: (+34) 964-728-066
E-mail: safont@exp.uji.es

Supporting information for this article is available on the WWW under http://dx.doi.org/10.1002/chem.200902233.

units have been widely investigated in our research group, motivated by the relevance of these cubane-type structures as models for several biological and industrial catalytic processes.[10,11] These investigations revealed the role of the solvent and counterion in the kinetics and mechanism of the proton-transfer reaction. Thus, the protonation of the hydride cubane-type cluster $[W_3Q_4H_3(dmpe)_3]^+$ (Q = S, Se; dmpe = 1,2-bis(dimethylphosphanyl)ethane) with HX (X = Cl, Br) in CH_3CN and CH_3CN/H_2O mixtures to form the corresponding $[W_3Q_4X_3(dmpe)_3]^+$ halide complexes [Eq. (2)] occurs with three kinetically distinguishable steps,[12,13] which include not only acid attack but also reaction with solvent molecules to form $[W_3Q_4H_3(solv)(dmpe)_3]^+$ intermediates. In contrast, kinetic studies on the reaction of $[W_3S_4H_3(dmpe)_3]^+$ with HCl in CH_2Cl_2 shows a second-order dependence on acid concentration and no intermediates with coordinated solvent are identified.

$$[W_3Q_4H_3(dmpe)_3]^+ + 3\,HX \rightarrow [W_3Q_4X_3(dmpe)_3]^+ + 3\,H_2 \quad (2)$$

Experimental and computational results revealed the existence of two competitive reaction pathways for protonation of the hydride ligands in CH_2Cl_2. Following the initial formation of a dihydrogen-bonded W–H···H–Cl adduct, one of the pathways consists of direct proton transfer within the W–H···H–Cl adduct to form W–Cl and H_2, whereas the other one requires the presence of a second HCl molecule to form a W–H···H–Cl···H–Cl adduct that transforms into W–Cl, H_2 and HCl in the rate-determining step, the role of both HX molecules being to form a network of hydrogen bonds that decreases the activation barrier for H_2 elimination. In addition, the kinetics and mechanism of proton transfer in dichloromethane are largely affected by the formation of ($[W_3S_4H_3(dmpe)_3]^+$, BF_4^-) ion pairs, in which BF_4^- approaches the cluster at the proximities of one of the coordinated hydrides.[14] Proton transfer in these ion pairs takes place more slowly than for the case of W–H···H–Cl adducts resulting from the unpaired cluster.

Recently, we reported a kinetic study of the proton-transfer reaction between $[W_3PdS_4H_3(dmpe)_3(CO)]^+$ ($\mathbf{1}^+$) and HCl to yield $[W_3PdS_4Cl_3(dmpe)_3(CO)]^+$ ($\mathbf{2}^+$) in CH_3CN/H_2O mixtures. The initial step involves acid attack with a first-order dependence with respect to the acid, and the $[W_3PdS_4(CH_3CN)_3(dmpe)_3(CO)]^+$ intermediate was identified by ESI-MS.[15] Interestingly, there is no reaction between $\mathbf{1}^+$ and HCl in neat acetonitrile, which strongly suggests an important role of water in the proton-transfer reaction.

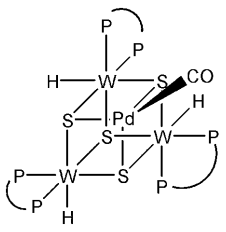

In the present work we extend the previous studies and report a kinetic and mechanistic study of the proton-transfer reaction using a weakly coordinating solvent such as CH_2Cl_2. Kinetic experiments show that cubane cluster $\mathbf{1}^+$ reacts with HCl in CH_2Cl_2 to yield $\mathbf{2}^+$ with a second-order dependence with respect to the acid, and no intermediate is identified experimentally. The kinetic effect of BF_4^- counterions is also reported. In addition computational studies aimed to elucidate the effect of changing the nature of the solvent on the mechanism of proton transfer are presented. The results indicate the relevance of the molecular interactions between cluster species and the solvent, as well as the possibility of formation of reaction intermediates with significant changes in the cluster. In this sense, we recently reported the operation of an open-core mechanism for ligand exchange on the copper atom in the $[W_3(CuCl)S_4H_3(dmpe)_3(CO)]^+$ cluster in which one Cu–S bond is elongated upon solvent attack.[16] The results in the present work suggest the existence of intermediates in the proton-transfer reaction in which coordination of a solvent molecule causes an increase of the coordination sphere of one tungsten atom and elongation of one Pd–W bond, which adds further support to an active role of the cluster core in the reactions of $M_3M'Q_4$ clusters.

Results and Discussion

Reaction kinetics of $\mathbf{1}^+$ with HCl in CH_2Cl_2: The kinetics of reaction of cluster $\mathbf{1}^+$ with acids in neat acetonitrile and acetonitrile–water has been reported previously,[15] and it was found that in those solvents the coordinating ability of acetonitrile allows the reaction to go through intermediates containing coordinated CH_3CN. As for the closely related trinuclear $[W_3S_4H_3(dmpe)_3]^+$ cluster,[12,17] it was found that the reaction in the less coordinating CH_2Cl_2 solvent proceeds through a different mechanism in which dihydrogen-bonded adducts evolve directly to the final product, we decided to study the kinetics of reactions of $\mathbf{1}^+$ with HCl in this solvent. The reaction of $\mathbf{1}^+$ with HCl in dichloromethane to form the trichlorocomplex $\mathbf{2}^+$ [Eq. (3)] occurs with spectral changes as those shown in Figure 1. The final spectrum shows a shoulder at about 520 nm and it coincides with that observed for $\mathbf{2}^+$ in $CH_3CN–H_2O$, thus showing that the spectrum of this species does not show significant changes with the nature of the solvent and that the spectral changes

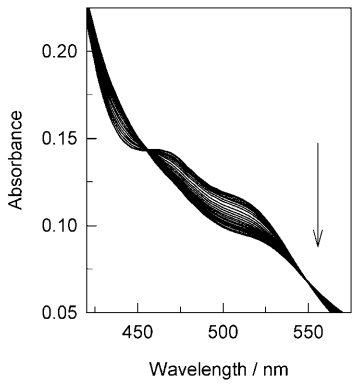

Figure 1. Spectral changes observed for the reaction of cluster $\mathbf{1}^+$ with HCl in CH_2Cl_2.

in Figure 1 correspond to complete conversion to the reaction product. A satisfactory fit of these spectral changes requires of three consecutive exponentials. The rate constants derived for the first step (k_{1obs}) show a clear second-order dependence with respect to the acid concentration (Figure 2), and a fit of the data by Equation (4) gives $k_1 = (1.84 \pm 0.07) \times 10^5\,\text{M}^{-2}\,\text{s}^{-1}$ at 25.0 °C.

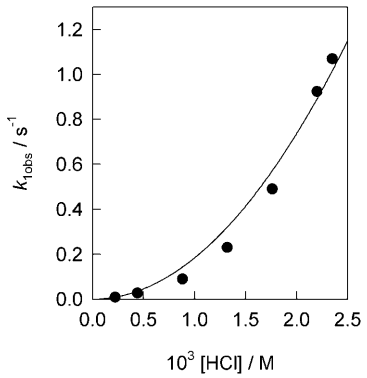

Figure 2. Plot of the dependence with respect to the acid concentration of the observed rate constant for the reaction of $\mathbf{1}^+$ with HCl (CH_2Cl_2, 25.0 °C).

$$\mathbf{1}^+ + \text{HCl(excess)} \rightarrow \mathbf{2}^+ + 3\,H_2 \quad (3)$$

$$k_{1obs} = k_1[\text{HX}]^2 \quad (4)$$

The dependence of the rate constants for the next two steps with the acid concentration is not so clear from the values of the observed rate constants deduced from the fitting procedure and so they will not be discussed in the paper. For the related trinuclear $[W_3S_4H_3(dmpe)_3]^+$ cluster,[12,17] a second-order dependence with respect to HCl could be deduced in CH_2Cl_2 for the first two steps, the third one also showing an undecipherable dependence with respect to the acid that converted to a second-order in experiments with added BF_4^-.[14] Thus, although no definitive conclusions can be obtained for the last two resolved steps in the kinetics of reaction in Equation (3), comparison with its closely related analogue makes reasonable the assumption that all the three steps are second-order with respect to HCl. In any case the value of k_1 above is close to that found for the reaction of $[W_3S_4H_3(dmpe)_3]^+$ with HCl in dichloromethane, for which $k_1 = (2.41 \pm 0.04) \times 10^5\,\text{M}^{-2}\,\text{s}^{-1}$,[12] thus showing that the introduction of the Pd(CO) fragment only leads to minor changes in the rate constants observed for the reaction with HCl in CH_2Cl_2, a conclusion similar to that previously derived in acetonitrile-containing solvent mixtures.[15]

The kinetic results for the reaction in Equation (3) can be rationalized on the basis of the mechanism previously proposed for $[W_3S_4H_3(dmpe)_3]^+$, which is depicted in Equations (5)–(8) for a single metal center.[17] The starting complex can interact with one or two HCl molecules to give W–H···H–Cl or W–H···H–Cl···H–Cl dihydrogen-bonded adducts in two rapid equilibria [Eqs. (5) and (6)]. These adducts can evolve to the reaction products through two competitive processes that are first- and second-order with respect to HCl, respectively [Eqs. (7) and (8)], but the experimental observation of a second-order dependence indicates that the contribution of the process in Equation (7) to the rate of reaction is negligible under the experimental conditions used. In that case the value of $k_1 = (1.84 \pm 0.07) \times 10^5\,\text{M}^{-2}\,\text{s}^{-1}$ corresponds to the product $K_{a1} \times K_{a2} \times k_4$. As pointed out previously for $[W_3S_4H_3(dmpe)_3]^+$,[17] formation of significant amounts of $(HCl)_2$ dimers in dichloromethane contributes, at least in part, to the second-order dependence with respect to HCl.

$$\text{W–H} + \text{H–Cl} \rightleftharpoons \text{W–H}\cdots\text{H–Cl} \quad K_{a1} \quad (5)$$

$$\text{W–H}\cdots\text{H–Cl} + \text{H–Cl} \rightleftharpoons \text{W–H}\cdots\text{H–Cl}\cdots\text{H–Cl} \quad K_{a2} \quad (6)$$

$$\text{W–H}\cdots\text{H–Cl} \rightarrow \text{W–Cl} + H_2 \quad k_3 \quad (7)$$

$$\text{W–H}\cdots\text{H–Cl}\cdots\text{H–Cl} \rightarrow \text{W–Cl}\cdots\text{HCl} + H_2 \quad k_4 \quad (8)$$

As a decelerating effect of added BF_4^- was observed for the reaction of $[W_3S_4H_3(dmpe)_3]^+$ with HCl in dichloromethane,[14] similar experiments were carried out for cluster $\mathbf{1}^+$. The results are illustrated in Figure 3 that shows a clear

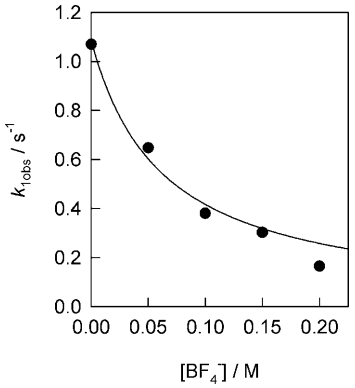

Figure 3. Plot showing the decrease in the value of k_{1obs} for the reaction of $\mathbf{1}^+$ with 2.4×10^{-2} M HCl (CH_2Cl_2, 25.0 °C) when the reaction is carried out in the presence of different concentrations of BF_4^-.

decrease of k_{1obs} when $[BF_4^-]$ increases. The experiments were carried out with a constant HCl concentration of 2.4×10^{-3} M and the data can be fitted by Equation (9) with $a = 1.09 \pm 0.06\,\text{s}^{-1}$ and $b = 16 \pm 2\,\text{M}^{-1}$. These results can be interpreted in terms of formation of a stable ($\mathbf{1}^+$, BF_4^-) ion pair that is unable to evolve to the reaction products. In that case the mechanism would be represented by adding Equation (10) to Equations (5)–(8), and the rate law would be given by Equation (11). The value of a coincides with the

rate constant measured for that concentration of acid in the absence of added BF_4^-, and b measures the equilibrium constant for the formation of the ion pair. The value of K_{BF_4} determined for $\mathbf{1}^+$ is one order of magnitude smaller than that previously determined for the $[W_3S_4H_3(dmpe)_3]^+$ cluster, for which K_{BF_4} is $7\times10^2\,M^{-1}$.[14] Although there is the possibility that the rate changes with added BF_4^- were caused by medium effects or by association of this anion with HCl to form a weaker acid, we favor the interpretation based on ion pairing because formation of ion pairs between this kind of cluster and BF_4^- has been previously demonstrated by using ^1H, ^{19}F-HOESY NMR spectra.[14]

$$k_{obs} = \frac{a}{1 + b[BF_4^-]} \tag{9}$$

$$W{-}H + BF_4^- \rightleftharpoons (W{-}H,\ BF_4^-) \qquad K_{BF_4} \tag{10}$$

$$k_{obs} = \frac{k_4 k_{a1} k_{a2}[HCl]^2}{1 + K_{BF4}[BF_4^-]} \tag{11}$$

Computational studies: To obtain additional information about the intimate details of the reaction mechanisms of proton transfer from HCl to cluster $\mathbf{1}^+$, DFT calculations were carried out using the theoretical model $[W_3Pd(CO)S_4H_3(PH_3)_6]^+$ ($\mathbf{3}^+$), in which the dmpe ligands are substituted by PH_3 in order to achieve reasonable computing times. For the same reasons, calculations were limited to reaction at a single W–H site. Calculations were initially carried out to understand the kinetics and reaction mechanism in CH_2Cl_2, in which a second-order dependence with respect to HCl and a deceleration in the presence of added BF_4^- is observed. As these calculations are similar to those previously described for the related $[W_3S_4H_3(PH_3)_6]^+$ cluster, the results will be only briefly commented. Additional calculations were carried out aimed to understand the different kinetics and reaction mechanism observed in acetonitrile–water solvent mixtures, in which three kinetic steps can be resolved for the reaction at each metal center and the formation of an intermediate containing coordinated acetonitrile is observed.[15] In this sense, the recent report[16] showing that formation of open-core cluster structures upon CH_3CN or H_2O attack can provide efficient alternative reaction pathways for the substitution of coordinated chloride in the $[W_3CuClS_4H_3(dmpe)_3]^+$ cluster provided an attractive starting point for the calculations.

Reaction mechanism between 3^+ and HCl in CH_2Cl_2: The theoretical approach for the reaction in dichloromethane assumes that the attacking species in the proton-transfer process is the HCl molecule. The formation of Cl^- or homoconjugated HCl_2^- species can be ignored, because of the low degree of dissociation of HCl in dichloromethane. Previously reported B3LYP/Lanl2DZ calculations have shown that the proton transfer to the hydrido $[W_3S_4H_3(PH_3)_6]^+$ cluster is clearly favored at the W–H bonds with respect to attack at the bridging sulfide ligands, even when two acid molecules are included in the calculations.[12,17] In this work, the interactions of one and two HCl molecules at different sites of the model complex $\mathbf{3}^+$ were computed in CH_2Cl_2 at the same level previously used for the trinuclear cluster. The results are summarized in Figure 4, which indicates that the

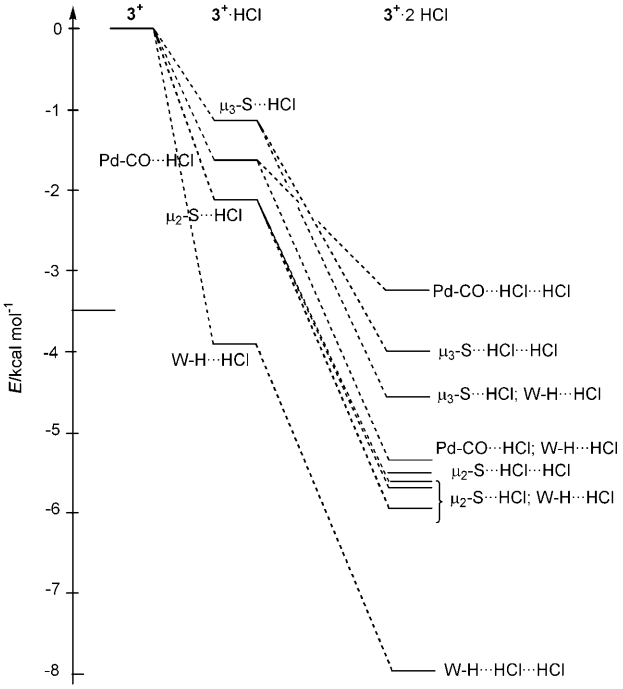

Figure 4. Reaction energies calculated in CH_2Cl_2 for the interaction of one and two HCl molecules at different sites of model cluster $\mathbf{3}^+$. All values are reported in Table S1 (see Supporting Information).

stabilization energy associated to the formation of the $\mathbf{3}^+$···HCl adduct is maximized when the interaction occurs with a coordinated hydride to form a dihydrogen-bonded W–H···H–Cl adduct, the stabilization achieved with interactions at the μ_2-S^{2-} or μ_3-S^{2-} ligands or the Pd(CO) fragments being lower. Similar conclusions are obtained when a second HCl molecule is included in the calculations, formation of the W–H···H–Cl···H–Cl adduct being clearly favored with respect to other possibilities in which both HCl molecules interact with the same or different centers of the cluster (see Figure 4). The optimized geometries for the W–H···H–Cl and W–H···H–Cl···H–Cl adducts are included in Figure 5, which shows that the interaction of the second HCl molecule causes a decrease of the H···H distance from 1.30 to 1.15 Å, so that the interaction with two HCl molecules makes the system more prepared for H_2 release.

Once established the geometries and energies of the adducts formed by $\mathbf{3}^+$ and HCl, the corresponding reaction products, $[W_3PdS_4ClH_2(PH_3)_6(CO)]^+$ ($\mathbf{4}^+$) and $\mathbf{4}^+$···HCl with the HCl molecule hydrogen bonded to the coordinated hydride, were optimized and their energies calculated in CH_2Cl_2. In both cases the reaction was found to be thermodynamically favored, as indicated graphically in Figure 6 and numerically in Table S2 (see Supporting Information). Figure 6 also shows the energy barriers associated to conver-

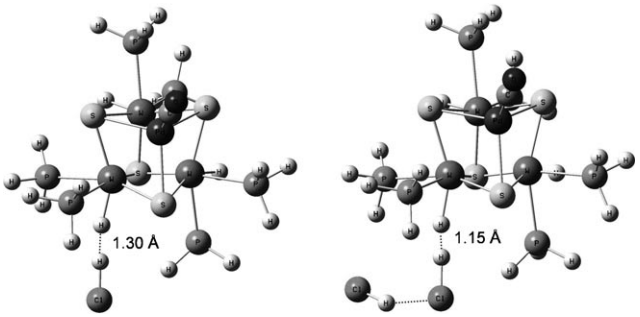

Figure 5. Optimized geometries and H···H distances for the most stable adducts formed by cluster $\mathbf{3}^{+}$ with one and two HCl molecules.

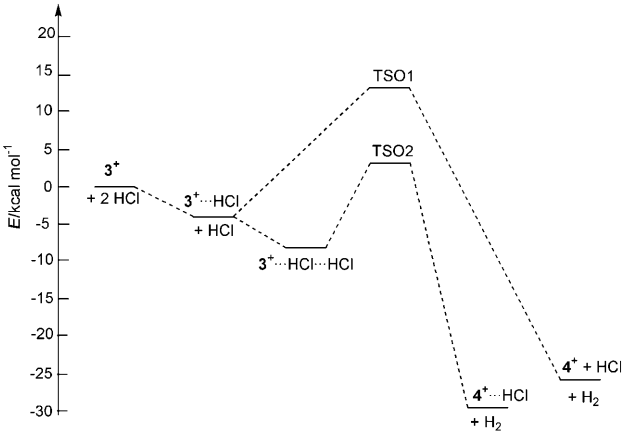

Figure 6. Energy profile showing the competitive first- and second- order pathways for the reaction between $\mathbf{3}^{+}$ and HCl. Note that, for consistency, two HCl molecules have been written for both pathways, although only one of them was used in the calculations corresponding to the upper pathway. Represented values have been calculated in CH_2Cl_2. All values are reported in Table S2 (see Supporting Information).

sion of the W–H···H–Cl and W–H···H–Cl···H–Cl adducts to the reaction products. The process occurs through transition states TSO1 and TSO2 (in which O1 and O2 refer to order 1 and 2, respectively), the geometries of which are shown in Figure 7. The structure of TSO1 can be described as a dihydrogen complex ion-paired to Cl^{-}, with a very short H–H distance (0.78 Å) and two non-equivalent W···H distances (2.19 and 2.33 Å), the activation barrier for this pathway (17.07 kcal mol^{-1}) being slightly higher (ca. 4 kcal mol^{-1}) than that described for $[W_3S_4H_3(PH_3)_6]^{+}$.[17] Conversion of the W–H···H–Cl···H–Cl adduct to the final product occurs through a transition state (TSO2) that can be described as a dihydrogen complex ion-paired with a HCl_2^{-} anion, with a H–H distance of only 0.76 Å and W–H distances of 2.57 and 2.69 Å. In agreement with the shorter H–H distance, the activation barrier for this pathway (11.29 kcal mol^{-1} in CH_2Cl_2) is lower than that involving TSO1, thus justifying the second-order dependence with respect the acid experimentally observed. It is interesting to note that the results of the DFT calculations for the $\mathbf{3}^{+}$ cluster clearly favor the second-order pathway (energy barriers of 17.07 and 11.29 kcal for pathways involving one and two HCl molecules, respectively), whereas for the related trinuclear $[W_3S_4H_3(dmpe)_3]^{+}$ cluster the energy barriers for both pathways were quite similar (13.38 and 12.23 kcal for one and two HCl molecules, respectively). Nevertheless, the second-order pathway is expected to be favored for both complexes provided there is HCl enough to allow for the formation of W–H···H–Cl···H–Cl adducts.

In order to explain the deceleration observed when the reaction with HCl is carried out in the presence of added BF_4^{-}, the geometry of the ($\mathbf{3}^{+}$, BF_4^{-}) ion pair was also optimized and it is shown in Figure 8. The anion approaches to the cluster at the proximities of one coordinated hydride,

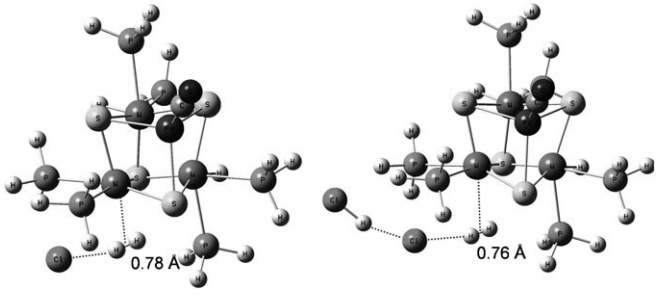

Figure 7. Optimized geometries for the transition states TSO1 and TSO2 calculated for the conversion to the final products of the W–H···H–Cl and W–H···H–Cl···H–Cl adducts resulting from the interaction of $\mathbf{3}^{+}$ with HCl. The H···H distances are expressed in the figure.

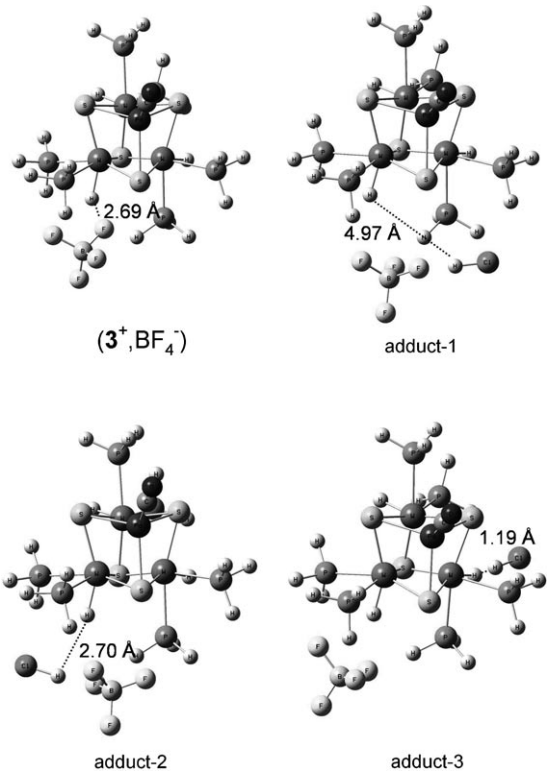

Figure 8. Optimized geometries for the ($\mathbf{3}^{+}$, BF_4^{-}) ion pair and the ($\mathbf{3}^{+}$, HCl, BF_4^{-}) adducts. Relevant distances are expressed in the figure.

the shortest H···F distance being 2.69 Å. Because of the simplification of the model, significant interactions between the F atoms of the anion and the hydrogens of PH_3 are also observed (shortest H···F distances of 1.90 and 1.95 Å) and they surely contribute to some extent to the docking of the anion. The ion pair is found to be 7.30 kcal mol^{-1} more stable than the separated ions. This energy is quite similar to that found for the BF_4^- ion pair formed by the trinuclear $[W_3S_4H_3(PH_3)_6]^+$ cluster (6.37 kcal mol^{-1}), so that the calculations are unable to explain the lower stability of the ($\mathbf{1}^+$, BF_4^-) ion pairs deduced from the K_{BF_4} values. With regards to the deceleration observed upon addition of BF_4^-, it was established for the related trinuclear cluster that it is caused by the formation of cluster–HCl–BF_4^- adducts in which ion-pairing and dihydrogen-bonding compete with each other, so that the most stable structures contain a BF_4^- ion placed at positions that make the H···H distance in the dihydrogen bond to increase up to values too large to allow formation of H_2.[14] To confirm this hypothesis, the corresponding adducts were also optimized for the case of the $\mathbf{3}^+$ cluster and the resulting geometries are also included in Figure 8. As for the case of the trinuclear cluster, two adducts with close values of energy were found. The species labeled adduct-1 and adduct-2 in Figure 8 are 16.57 and 17.31 kcal more stable in CH_2Cl_2 than the three separate components, the values for the corresponding species in the case of the trinuclear cluster being quite similar (15.64 and 15.76 kcal, respectively). The large H···H distances in these species (4.97 and 2.70 Å in adduct-1 and adduct-2, respectively) make them a dead-end in the mechanism of proton transfer to the coordinated hydride and the reaction must go through alternative pathways, such as that involving adduct-3 in Figure 8 in which the dihydrogen bond with the HCl molecule is formed with a W–H bond different from the one interacting with BF_4^-. Nevertheless, adduct-3 is 2.15 and 2.38 kcal mol^{-1} less stable than adducts-1 and -2 respectively, so that it will be only a minor species in solution and the rate of reaction will result significantly decreased. Thus, it appears that for this kind of cluster ion pairing to BF_4^- decreases the rate of proton transfer to the coordinated hydride because the BF_4^- competes with HCl in the interaction with the coordinated hydride, a behavior different from that observed for the reaction of *trans*-$[FeH(H_2)(dppe)_2]^+$ with NEt_3, in which the BF_4^- follows the proton along the proton transfer, thus making the reaction to go faster in the presence of this anion.[18,19]

Calculations on the reaction between $\mathbf{3}^+$ and HCl in neat CH_3CN: The simplest approach to the mechanism of reaction in acetonitrile is to consider the reaction pathways discussed above for CH_2Cl_2. In this way, the energy profiles calculated for the pathways involving one and two HCl molecules by application of the polarizable continuum model (PCM) in acetonitrile are quite similar to those obtained in dichloromethane. Thus, the stabilization achieved for the formation of the reaction products and the energy barriers through the transition states TSO1 and TSO2 are very similar in both solvents (see Figure S1 in the Supporting Information), which suggests that reaction between $\mathbf{1}^+$ and HCl in CH_3CN should occur through the same pathway observed in dichloromethane. However, these results are unable to explain the previously reported absence of reaction between $\mathbf{1}^+$-PF_6^- and HCl in neat acetonitrile[15] and so it must be concluded that the lack of reaction is caused by a factor not considered in those calculations.

The major goal to be achieved with additional calculations in neat acetonitrile would be thus to explain the absence of reaction between $\mathbf{3}^+$ and HCl in this solvent despite the occurrence of the process in dichloromethane and the similarity of the energy profiles calculated for proton transfer in CH_3CN and CH_2Cl_2. Although the calculations described above take into account solvent effects by using the PCM method, it is evident that specific interactions of the reagents with solvent molecules can modify substantially the energy profiles, especially in the case of good donor solvents as acetonitrile. It is important to note that in order to start the proton transfer, an M–H···H–X dihydrogen bond must be formed from $(M–H)_{solv}$ and $(H–X)_{solv}$, and this process requires significant rearrangement of the solvent molecules at the proximities of the dihydrogen bond. In particular, any solvent molecule placed along the direction defined by the two hydrogen atoms must be displaced in order to allow for the short H···H distance required for the formation of a dihydrogen bond able to evolve to the reaction products. The energy required for such reorganization is expected to change significantly depending on the nature of the reagents and the solvent, being most important in cases where there is a strong interaction of the solvent with at least one of the reagents. One clear case is that of the interaction of an acid as HCl with solvents as CH_3CN and CH_2Cl_2, the interaction with acetonitrile being expected to be significantly stronger than with dichloromethane. A simple way of estimating this effect is calculating the energy change associated to the interaction of HCl with a single solvent molecule [Eq. (12)].

$$\mathrm{HCl} + \mathrm{solv} \rightleftharpoons \mathrm{solv{-}HCl} \qquad (12)$$

The calculations were made optimizing the solv–HCl species for solv = CH_2Cl_2 and CH_3CN in the gas phase and then applying the PCM method in the corresponding solvent. In the case of CH_2Cl_2 different optimizations were made assuming formation of adducts with either HCl···$HCCl_2H$ or ClH···$ClCClH_2$ interactions, but in both cases they led to a minimum for a structure of the type ClH···$ClCClH_2$. The results indicate that the stabilization achieved with the interaction of HCl with a molecule of CH_3CN is of 9.14 kcal mol^{-1}, but is only of 1.68 kcal mol^{-1} in CH_2Cl_2. From these values, it is expected that whereas the energy profiles discussed above will not change significantly in dichloromethane, the picture will change in the case of acetonitrile, in which the CH_3CN···HCl interaction is stronger than M–H···H–X and introduces a contribution that hinders formation of the dihydrogen bond. Nevertheless, this conclusion must be taken with care because the solvent molecule in CH_3CN···HCl can

interact with the dihydrogen-bonded species and the corresponding stabilization energy may cancel, at least partially, the energy cost required for breaking the specific solv–HCl interaction.

To obtain more information about the effect of solvation, additional calculations were made considering one solvent molecule interacting with each one of the reagents involved in the formation of the dihydrogen bond. The calculations were carried out for both $\mathbf{3}^+$ and HCl interacting with one molecule of CH_2Cl_2 or CH_3CN placed at the proximities of the W–H or H–Cl bonds. In order to estimate the energy changes associated to the reorganization of the solvent molecules upon formation of the dihydrogen bond, the geometry of the dihydrogen-bonded $\mathbf{3}^+\cdots$HCl species was also optimized with two solvent molecules placed at the proximities of the dihydrogen bond. Those calculations indicated that neither the CH_2Cl_2 nor the CH_3CN molecules interact significantly with the coordinated hydride, the optimized geometries of $\mathbf{3}^+\cdots$solv showing the solvent molecule placed away from the W–H bond and the stabilization energy being only of 2.88 (CH_2Cl_2) or 2.40 kcal mol^{-1} (CH_3CN). These structures are reported in the supplementary material. With respect to the calculations involving the W–H···H–Cl···2 solv species, the results differ significantly for both solvents. For CH_2Cl_2 there is a weak interaction that results in an stabilization energy of only 3.18 kcal mol^{-1}, and the optimized geometry (see Figure 9) indicates that the H···H distance in

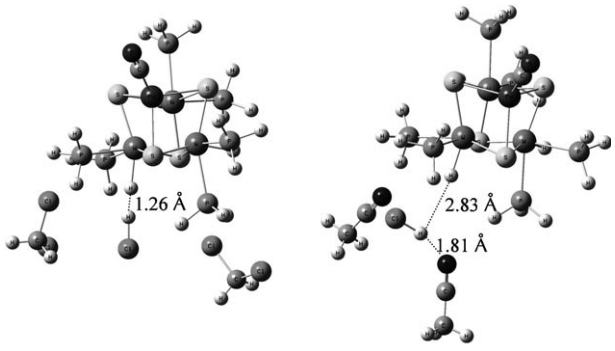

Figure 9. Geometries resulting from optimization of the dihydrogen bonded $\mathbf{3}^+\cdots$HCl species interacting with two molecules of CH_2Cl_2 and CH_3CN, respectively.

the dihydrogen bond does not change significantly upon inclusion of the two solvent molecules (1.26 vs 1.30 Å in the absence of solvent molecules). As the stabilization energy for this species (3.18 kcal mol^{-1}) is close to that achieved for the interaction of one solvent molecule with each one of the M–H and HCl species (4.56 kcal mol^{-1}), it can be concluded that consideration of specific interactions with solvent molecules are not expected to change significantly the energy profiles for proton transfer in CH_2Cl_2 shown in Figure 6.

In contrast, the results are very different when the calculations are carried out with two acetonitrile molecules. Although the stabilization energy (7.48 kcal mol^{-1}) is only a few kcal smaller than that achieved with the interaction with the separate reagents (11.54 kcal mol^{-1}), the H···H distance in the dihydrogen bond increases to a value (2.83 Å) that hinders proton transfer. These results clearly show that the consideration of specific interactions with acetonitrile molecules will make unviable in this solvent the reaction pathways in Figure 6, thus justifying the absence of reaction observed experimentally.

The reaction between $\mathbf{3}^+$ and HCl in CH_3CN/H_2O mixtures: In contrast to the absence of reaction in neat acetonitrile, kinetic experiments showed that $\mathbf{1}^+$-PF_6^- reacts with HCl in CH_3CN:H_2O (1:1) mixtures to give $\mathbf{2}^+$, although the process occurs with three resolved kinetic steps.[15] The first step (k_{1obs}) shows a first-order dependence with respect to the acid and leads to the formation of $[W_3PdS_4(CH_3CN)_3(dmpe)_3(CO)]^{4+}$ as the reaction intermediate, a proposal made on the basis of NMR results and kinetic data with other acids in neat CH_3CN. Following this initial step there are additional absorbance changes that lead to the spectrum of $\mathbf{2}^+$, although the kinetic analysis reveals that the process occurs with two resolved steps (k_{2obs} and k_{3obs}) both of them independent of the acid concentration. The absorbance changes corresponding to the k_{2obs} step are very small and limited to a short wavelength range, and they were interpreted as corresponding to some unknown secondary process. Nevertheless, it must be pointed out that for the closely related $[W_3S_4H_3(dmpe)_3]^+$ cluster the nature of the intermediate formed in the second resolved kinetic step was demonstrated to be the corresponding $[W_3S_4(H_2O)_3(dmpe)_3]^{4+}$ aqua cluster[12] and so, the possibility of formation of a similar triaqua cluster cannot be ruled out in the case of the Pd compound. The third resolved kinetic step leads in all cases to the formation of the final trichloro complex. Additional calculations were made aimed to explain these experimental observations, in particular the occurrence of reaction in acetonitrile–water mixtures and the change in the kinetics of reaction with respect to that observed in CH_2Cl_2.

The calculations described in the previous section clearly show that the HCl molecule is unable to transfer the proton to the coordinated hydride of $\mathbf{1}^+$ in neat acetonitrile, because the stability achieved with the formation of the W–H···H–Cl dihydrogen bond is unable to compensate the interaction of HCl with solvent molecules, and a similar situation is expected to occur in acetonitrile–water mixtures. However, in the latter solvent mixtures the HCl molecule is dissociated with formation of solvated Cl^- and H^+, so that the protonating agent must be the solvated proton. Although in 1:1 acetonitrile–water solvent mixtures the proton can interact with molecules of both co-solvents, preferential solvation with water is expected to occur because with respect to proton acetonitrile is a much weaker base than water,[20,21] and actually there is experimental evidence supporting the preferential interaction of protons with a varying number of water molecules.[22–24] For simplicity, H_3O^+ was

chosen as a model in the calculations, which were performed in all cases by optimizing geometries in the gas phase followed by consideration of the solvent effect by making PCM calculations in both CH_3CN and H_2O. However, for simplification the results will be discussed using in all cases the mean value of the energies obtained in both solvents, which can be considered a reasonable estimation of the energies in 1:1 acetonitrile/water mixtures.[16] To simplify the presentation, the results of calculations regarding acid attack to the coordinated hydride to give species with coordinated acetonitrile or water, and those involving substitution of coordinated solvent by Cl^- will be discussed separately.

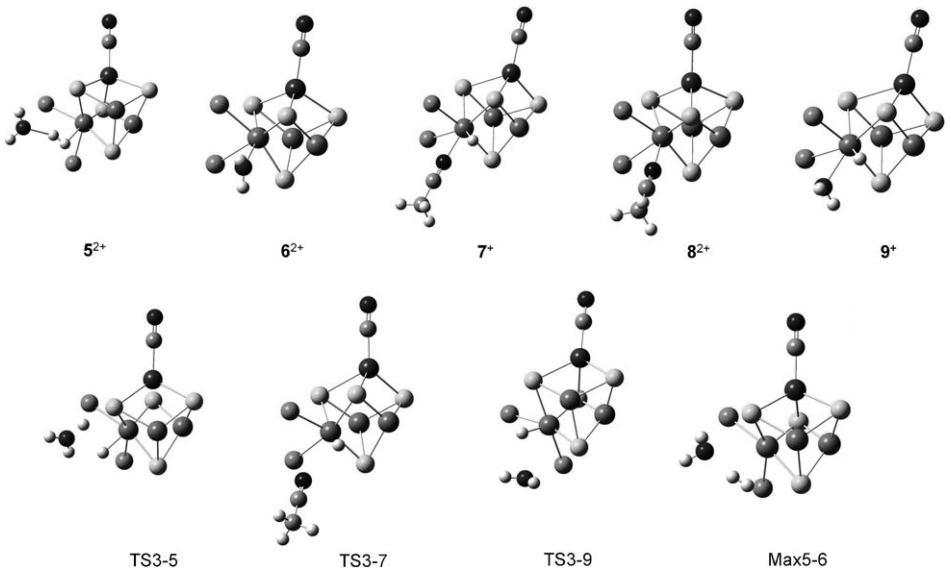

Figure 10. Gas-phase-optimized structures of the species involved in proton transfer to the coordinated hydrides of $\mathbf{3}^+$ in acetonitrile–water solvent mixtures (see the energy profiles in Figure 11). Hydrogen atoms and phosphine ligands for the non-active tungsten atoms have been omitted for clarity.

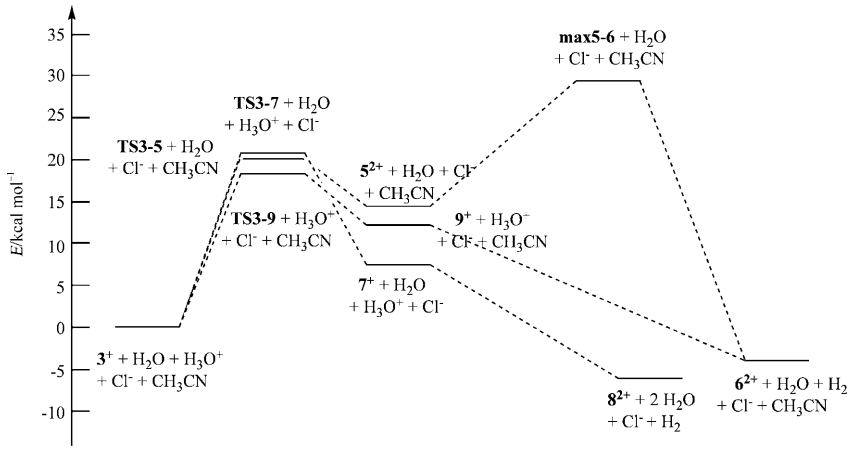

Figure 11. Energy profiles for the attack of H_3O^+, H_2O and CH_3CN to cluster $\mathbf{3}^+$ with formation of compounds containing coordinated water ($\mathbf{6}^{2+}$) and coordinated acetonitrile ($\mathbf{8}^{2+}$).

According to the calculations, attack of H_3O^+ to one of the coordinated hydrides of $\mathbf{3}^+$ leads to formation of intermediate $[W_3PdS_4H_3(H_3O)(PH_3)_6(CO)]^{2+}$ ($\mathbf{5}^{2+}$), the structure of which can be described as a dihydrogen complex hydrogen bonded to a water molecule (see Figure 10). The H–H distance is 0.79 Å, whereas the W–H distances are 1.99 and 2.22 Å. Formation of this intermediate occurs through transition state **TS3–5** (see geometry in Figure 10 and energy profile in Figure 11) with an energy barrier of 20.6 kcal mol^{-1} in 1:1 CH_3CN:H_2O (13.7 and 27.4 kcal mol^{-1} in neat acetonitrile and water, respectively). From intermediate $\mathbf{5}^{2+}$ the reaction can proceed with substitution of coordinated H_2 by the water molecule, and scan calculations indicate that it occurs with an additional barrier of 14.6 kcal mol^{-1} in the mixed solvent (14.7 and 14.5 kcal mol^{-1} in neat acetonitrile and water, respectively). The result of the substitution process is intermediate $[W_3PdS_4H_2(H_2O)(PH_3)_6(CO)]^{2+}$ ($\mathbf{6}^{2+}$), which has a structure similar to the starting compound except that the hydride has been replaced by a water ligand. It is interesting to note that intermediate $\mathbf{5}^{2+}$ represents the first case in which theoretical calculations with this kind of cluster lead to a structure typical of dihydrogen complexes as stable intermediate, although they use to appear as transition states (see for example transition states TSO1 and TSO2 in Figure 7). However, we have been unable to obtain any experimental evidence on the formation of dihydrogen complexes as intermediates with any of the hydride clusters studied to date. In addition, kinetic studies[15] indicate that the conversion of the starting complex to the acetonitrile-containing intermediate occurs in a single step. For these reasons, if reaction with HCl in acetonitrile–water mixtures were through this mechanism, it should be assumed that conversion of $\mathbf{3}^+$ to $\mathbf{6}^{2+}$ occurs in a single step with a barrier of 29.4 kcal mol^{-1} (21.9 and 36.9 kcal mol^{-1} in neat acetonitrile and water, respectively). The subsequent conversion of $\mathbf{6}^{2+}$ to the final chloro complex will be discussed below.

Although the reaction pathway in the previous paragraph is not exceedingly energy demanding, the recent report of the possibility of generating open-core cluster structures by

acetonitrile or water attack to the $[W_3CuS_4]$ cluster[16] led us to consider an alternative pathway involving direct acetonitrile attack to cluster $\mathbf{3}^+$ to generate a species that retains the hydride but contains a coordinated CH_3CN, namely $[W_3PdS_4(CH_3CN)H_3(PH_3)_6(CO)]^+$ ($\mathbf{7}^+$). The coordination number of the reactive tungsten center, without considering the metal–metal bonds, increases from six in complex $\mathbf{3}^+$ to seven in $\mathbf{7}^+$ (see the optimized geometry in Figure 10). The W–H bond length in compound $\mathbf{7}^+$ is 1.70 Å, so that it is not significantly affected by coordination of the nitrile ligand. The P-W-H angle increases from 72.06 to 134.76°, whereas the S-W-S angles in the same coordination plane decrease from 111.09 to 81.44°. In addition, the W–Pd bond length increases from 2.99 in $\mathbf{3}^+$ to 3.84 Å in $\mathbf{7}^+$, thus leading to further distortion of the cubane cluster unit. However, the W–S bond lengths and one of the Pd–S distances closer to the center of reaction increase only by about 0.1 Å, in opposition to the larger Cu–S bond elongation observed in open-core species derived from the $[W_3CuClS_4H_3(dmpe)_3]^+$ cluster.[16] Formation of $\mathbf{7}^+$ occurs through transition state **TS3–7** (see geometry in Figure 10 and energy profile in Figure 11) with an energy barrier of 20.6 kcal mol^{-1} in 1:1 CH_3CN:H_2O (20.0 and 21.2 kcal mol^{-1} in neat acetonitrile and water, respectively), and the relative energy of $\mathbf{7}^+$ with respect to $\mathbf{3}^+ + CH_3CN$ is 7.3 kcal mol^{-1} (7.1 and 7.5 kcal mol^{-1} in neat acetonitrile and water, respectively), thus showing that significant amounts of $\mathbf{7}^+$ are not expected to be formed in neat acetonitrile. However, H_3O^+ attack to this intermediate leads to formation of the acetonitrile complex without any additional energy barrier, so that the energy profile for this pathway in Figure 11 indicates that formation of $[W_3PdS_4(CH_3CN)H_2(PH_3)_6(CO)]^{2+}$ ($\mathbf{8}^{2+}$, see Figure 10), which represents the experimentally detected $[W_3PdS_4(CH_3CN)_3(dmpe)_3(CO)]^{4+}$ intermediate, occurs with a single activation barrier, thus supporting the operation of this mechanism for the initial proton transfer to the coordinated hydride. A similar reaction pathway can be obtained by considering an initial attack of water to $\mathbf{3}^+$ to give intermediate $\mathbf{9}^+$, which contains hydride and water coordinated simultaneously to the same metal center. This attack occurs through **TS3–9** with an activation barrier of 18.6 kcal mol^{-1} (18.1 and 19.0 in CH_3CN and H_2O, respectively). The intermediate $\mathbf{9}^+$ is 4.7 kcal mol^{-1} less stable than $\mathbf{7}^+$ in CH_3CN–H_2O mixtures, and it converts to the aqua complex $\mathbf{6}^+$ without additional barrier.

According to the calculations, the pathways in Figure 11 involving CH_3CN and H_2O attacks do not differ very much in energy, so that the intermediates $\mathbf{8}^{2+}$ and $\mathbf{6}^+$ containing coordinated acetonitrile and water, respectively, are expected to be formed. Although we have no experimental evidence (ESI-MS and NMR spectroscopy) on the formation of aqua complexes as intermediates in experiments carried out in CH_3CN/H_2O mixtures, the possibility of formation of small amounts of this complex cannot be completely ruled out and, actually, they could be the responsible of the minor spectral changes observed in the second resolved kinetic step in acetonitrile–water solvent mixtures. In view of the present results, the detection of the aqua intermediate in the reaction of the closely related $[W_3S_4H_3(dmpe)_3]^+$ cluster appears to indicate that the relative energies of both pathways in Figure 11 can change when the structure of the cluster is modified.

Once $\mathbf{8}^{2+}$ is formed, the acetonitrile ligand has to be substituted by the chloride. To investigate this process, a bidimensional scan taking as reference coordinates the W–Cl and W–$NCCH_3$ distances was carried out. From the potential energy surface (Figure 12) obtained in this way it can be

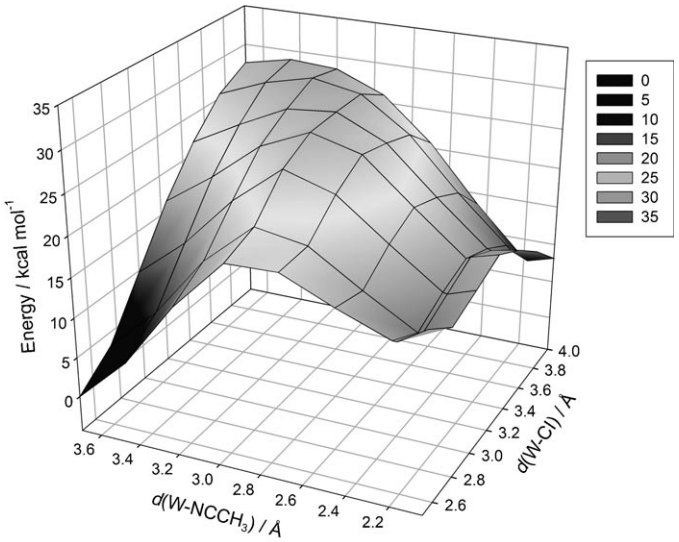

Figure 12. Potential energy surface calculated for the substitution of acetonitrile by chloride in cluster $\mathbf{8}^+$.

deduced that the process connecting $\mathbf{8}^{2+}$ with $\mathbf{4}^+$ is a two-step process passing through an intermediate with small values for both distances. Hence, the substitution mechanism appears to involve chloride attack to $\mathbf{8}^{2+}$ to give the $[W_3PdS_4(CH_3CN)ClH_2(PH_3)_6(CO)]^+$ ($\mathbf{10}^+$, see Figure 13) intermediate, which finally dissociates the acetonitrile ligand to give the reaction product $\mathbf{4}^+$. Complex $\mathbf{10}^+$ is isostructural to $\mathbf{7}^+$, with W–Pd, W–N, and W–Cl bond lengths of 3.82, 2.18, and 2.69 Å, respectively, and its formation reveals that

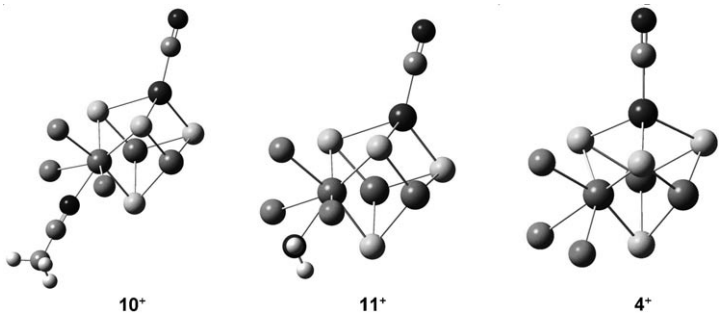

Figure 13. Gas-phase-optimized structures of intermediates $\mathbf{10}^+$ and $\mathbf{11}^+$ and product $\mathbf{4}^+$. Hydrogen atoms and phosphine ligands for the non-active tungsten atoms have been omitted for clarity.

structural changes in the cluster core can also provide efficient reaction pathways for this substitution. The cubane-type cluster structure is recovered for $\mathbf{4}^{+}$, with W–Pd and W–Cl bond lengths of 3.04 and 2.53 Å, respectively. Figure 14 depicts the energy profile for the substitution process. Intermediate $\mathbf{10}^{+}$ lies 1.2 kcal mol^{-1} over $\mathbf{8}^{2+}$, and the activation barrier on the passage from $\mathbf{8}^{2+}$ to $\mathbf{10}^{+}$ is of 3.7 kcal mol^{-1}. On the other hand, the reaction product $\mathbf{4}^{+}$ lies 20.7 kcal mol^{-1} below $\mathbf{8}^{2+}$, and the activation barrier on going from $\mathbf{10}^{+}$ to $\mathbf{4}^{+}$ is of 7.4 kcal mol^{-1}.

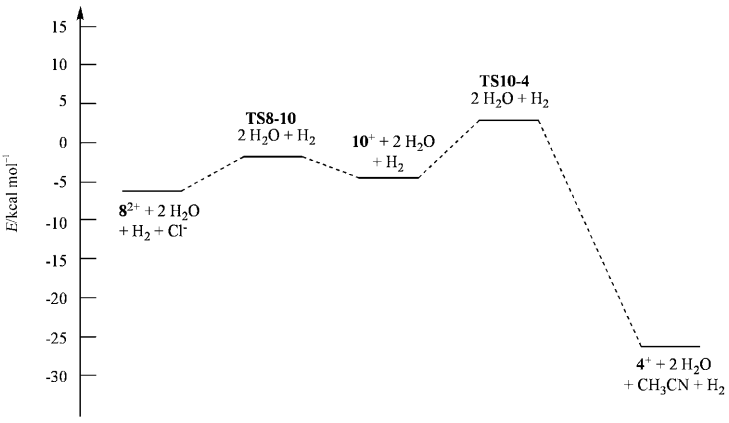

Figure 14. Reaction profile for the substitution process occurring at the latter stages of the reaction between the hydride cluster and HCl in acetonitrile–water solvent mixtures.

Conclusions

The experimental and theoretical results obtained for the $[W_3S_4H_3(dmpe)_3Pd(CO)]^{+}$ cluster illustrate the rich mechanistic chemistry of proton transfer from acids to the coordinated hydride in this kind of cluster. A variety of mechanistic pathways can operate depending on the nature of the acid, solvent and the presence of external anions (see Figure 15). Thus, in solvents of low dielectric constant, such as dichloromethane, acids exist in molecular form (for example HCl) and reaction goes through the initial formation of a dihydrogen bonded adduct that evolves to the reaction product in the rate determining step. This pathway is in competition with another one in which the product is formed through an adduct with two acid molecules (pathway b in Figure 15), so that kinetic studies reveal that the reaction occurs in a single step which is first- or second-order with respect to the acid depending on which pathway dominates. In this kind of solvent the cationic clusters have a high tendency to form ion pairs with external anions as BF_4^{-};[14] although ion pairs have been found to provide efficient reaction pathways for proton transfer in other complexes,[18] in these clusters formation of ion pairs hinders proton transfer and so they represent dead-end in the reaction (pathway c in Figure 15), which is signalled in kinetic studies by a decrease in the rate of reaction. When the reaction is carried out in a solvent of higher basicity as acetonitrile, there are stronger interactions between the acid molecule and the solvent that, at least in cases as HCl, cannot be compensated with the stabilization achieved with formation of a dihydrogen bond, which makes pathways a and b in Figure 15 inoperative. Although in the present case the cluster does not react with HCl in acetonitrile, there is reaction with other acids and also there are other clusters that do react with HCl in this solvent; in those cases the reaction can go through intermediates with open-core cluster structure resulting from solvent attack to the metal center (pathways d and e in Figure 15), a type of pathway recently proposed to be operative in reactions of these clusters. Finally, when the reaction is carried out in acetonitrile–water solvent mixtures the attacking species is the solvated proton, which can carry out the proton transfer to coordinated hydride through two alternative mechanisms: direct attack to the coordinated hydride (pathway e in Figure 15) or through attack to an open-core intermediate resulting from solvent attack (pathway f in Figure 15). In these cases, the result of proton attack is a cluster containing a coordinated solvent molecule that can be replaced by the anion of the acid in subsequent substitution processes. As a consequence, kinetic studies reveal in those cases a polyphasic kinetics in which only the initial step is dependent on the concentration of the acid.

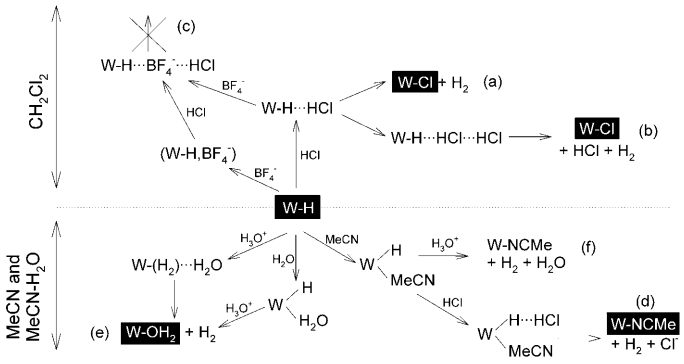

Figure 15. Alternative pathways for proton transfer from acids to coordinated hydride in $[W_3PdS_4H_3(dmpe)_3(CO)]^{+}$ and related clusters.

Experimental Section

Synthesis and physical measurements: Compound $\mathbf{1}^{+}$-PF_6^{-} was prepared as previously described.[15] $^{31}P\{^1H\}$ NMR spectra were recorded on a Varian Unity 400 spectrometer and they were referenced to external 85% H_3PO_4. ^1H and $^{13}C\{^1H\}$ Spectra were recorded on a Varian Inova 500 spectrometer, the chemical shifts being reported in ppm from tetramethylsilane with the solvent resonance taken as the internal standard.

Kinetic experiments: The kinetics of the reaction of the $\mathbf{1}^{+}$ cluster with acids was studied by using an Applied Photophysics SX17MV stopped-flow instrument provided with a PDA1 photodiode array (PDA) detector, and the data were analysed with the SPECFIT program using the appropriate kinetic model.[25] The experiments were carried out at 25.0 °C using neat CH_2Cl_2 as solvent and pseudo first-order conditions of acid excess by mixing solutions of the cluster compound and the acid. For experiments in the presence of Et_4NBF_4 this salt was added to the cluster

solution before mixing it with the acid in the stopped-flow instrument. The concentrations of acid were determined by extracting an aliquot (5 mL) of the CH_2Cl_2 solution with an excess of water (50 mL) and then titrating the water solution with a previously standardized KOH solution.

Theoretical calculations: The calculations were performed with the Gaussian 03 package[26] at the B3LYP level.[27,28] All atoms were represented by the relativistic core potential (LanL2) from Los Alamos with associated double-z pseudo-orbital basis set.[29] The geometry optimizations were performed without any symmetry constraint followed by analytical frequency calculations to confirm that a minimum or a transition state had been reached. For the case of transition states, once this vector was characterized, it was possible to trace the intrinsic reaction coordinate[30] path connecting each transition structure with the two associated minima by using the second-order González-Schlegel integration method.[31,32] The energies of all the systems studied at the B3LYP level in the gas phase were recomputed with single-point calculations by inclusion of solvent effects of dichloromethane ($\varepsilon = 8.93$), acetonitrile ($\varepsilon = 36.64$) and water ($\varepsilon = 78.39$) according to the polarizable continuum model (PCM) scheme as implemented in Gaussian, and the united atom topological model with UAHF radii was used.[33,34] Energies in CH_3CN:H_2O (1:1) mixtures were estimated as the average of computed energies in acetonitrile and in water solvents. Electronic PCM energies E and not Gibbs energies G are used for characterizing the reaction paths, due to the difficulties in calculating entropy in condensed phases. Several alternatives have been suggested in the literature, some of them even fully neglecting translational entropy, which is the greatest contribution to the total entropy term.[35–39]

Acknowledgements

This work was supported by the Spanish Ministerio de Educación y Ciencia (Projects CTQ2006-15447-C02-01 and CTQ2006-14909-C02-01), Ministerio de Ciencia e Innovación (Project CTQ2008-02670/BQU), Junta de Andalucía (Project P07-FQM-02734), Generalitat Valenciana (Projects ACOMP/2009/121 and PROMETEO/2009/053) and Fundació Bancaixa-Universitat Jaume I (Grants P1.1B2007-12 and P1.1B2008-37). A.G.A. acknowledges a predoctoral grant from the Spanish Ministerio de Ciencia y Tecnología. The authors also thank the Servei d'Informàtica of the Universitat Jaume I and the Servicios Centrales de Ciencia y Tecnología of the Universidad de Cádiz for providing us with the NMR and computing facilities.

[1] P. E. M. Siegbahn, J. W. Tye, M. B. Hall, *Chem. Rev.* **2007**, *107*, 4414.
[2] L. M. Epstein, E. S. Shubina, *Coord. Chem. Rev.* **2002**, *231*, 165.
[3] M. Peruzzini, R. Poli in *Recent Advances in Hydride Chemistry*, Elsevier, Amsterdam, **2001**.
[4] G. J. Kubas, *Metal Dihydrogen and σ-Bond Complexes*, Kluwer Academic/Plenum Publishers, New York, **2001**.
[5] G. J. Kubas, *Chem. Rev.* **2007**, *107*, 4152.
[6] M. Besora, A. LLedos, F. Maseras, *Chem. Soc. Rev.* **2009**, *38*, 957.
[7] E. Clot, *Eur. J. Inorg. Chem.* **2009**, 2319.
[8] G. Kovács, G. Ujaque, A. LLedos, *J. Am. Chem. Soc.* **2008**, *130*, 853.
[9] N. V. Belkova, T. N. Gribanova, E. I. Gutsul, R. M. Minvaev, C. Bianchini, M. Peruzzini, F. Zanobini, E. S. Shubina, L. M. Epstein, *J. Mol. Struct.* **2007**, *825–846*, 844.
[10] R. Hernández-Molina, A. G. Sykes, *J. Chem. Soc. Dalton Trans.* **1999**, 3137.
[11] R. Llusar, S. Uriel, *Eur. J. Inorg. Chem.* **2003**, 1271.
[12] M. G. Basallote, M. Feliz, M. J. Fernández-Trujillo, R. Llusar, V. S. Safont, S. Uriel, *Chem. Eur. J.* **2004**, *10*, 1463.
[13] M. G. Basallote, F. Estevan, M. Feliz, M. J. Fernández-Trujillo, D. A. Hoyos, R. Llusar, S. Uriel, C. Vicent, *Dalton Trans.* **2004**, 530.
[14] A. G. Algarra, M. G. Basallote, M. J. Fernández-Trujillo, R. Llusar, V. S. Safont, C. Vicent, *Inorg. Chem.* **2006**, *45*, 5774.
[15] A. G. Algarra, M. G. Basallote, M. Feliz, M. J. Fernández-Trujillo, E. Guillamón, R. Llusar, C. Vicent, *Inorg. Chem.* **2006**, *45*, 5576.
[16] A. G. Algarra, M. Feliz, M. J. Fernández-Trujillo, R. Llusar, V. S. Safont, C. Vicent, M. G. Basallote, *Chem. Eur. J.* **2009**, *15*, 4582.
[17] A. G. Algarra, M. G. Basallote, M. Feliz, M. J. Fernández-Trujillo, R. Llusar, V. S. Safont, *Chem. Eur. J.* **2006**, *12*, 1413.
[18] M. G. Basallote, M. Besora, J. Durán, M. J. Fernández-Trujillo, A. LLedos, M. A. Máñez, F. Maseras, *J. Am. Chem. Soc.* **2004**, *126*, 2320.
[19] M. G. Basallote, M. Besora, C. E. Castillo, M. J. Fernández-Trujillo, A. LLedos, F. Maseras, M. A. Máñez, *J. Am. Chem. Soc.* **2007**, *129*, 6608.
[20] J. F. Coetzee, D. K. McGuire, *J. Phys. Chem.* **1963**, *67*, 1810.
[21] I. M. Kolthoff, M. K. Chantooni, *J. Am. Chem. Soc.* **1968**, *90*, 3320.
[22] A. Wakisaka, Y. Shimizu, N. Nishi, K. Tokumaru, H. Sakuragi, *J. Chem. Soc. Faraday Trans.* **1992**, *88*, 1129.
[23] E. A. Quadrelli, H.-B. Kraatz, R. Poli, *Inorg. Chem.* **1996**, *35*, 5154.
[24] M. K. Chantooni, I. M. Kolthoff, *J. Am. Chem. Soc.* **1970**, *92*, 2236.
[25] SPECFIT-32, R. A. Binstead, B. Jung, A. D. Zuberbühler, Spectrum Software Associates, Chappel Hill, **2000**.
[26] Gaussian 03, Revision B.04, M. J. Frisch, G. W. Trucks, H. B. Schlegel, G. E. Scuseria, M. A. Robb, J. R. Cheeseman, J. A. Montgomery Jr., T. Vreven, K. N. Kudin, J. C. Burant, J. M. Millam, S. S. Iyengar, J. Tomasi, V. Barone, B. Mennucci, M. Cossi, G. Scalmani, N. Rega, G. A. Petersson, H. Nakatsuji, M. Hada, M. Ehara, K. Toyota, R. Fukuda, J. Hasegawa, M. Ishida, T. Nakajima, Y. Honda, O. Kitao, H. Nakai, M. Klene, X. Li, J. E. Knox, H. P. Hratchian, J. B. Cross, C. Adamo, J. Jaramillo, R. Gomperts, R. E. Stratmann, O. Yazyev, A. J. Austin, R. Cammi, C. Pomelli, J. W. Ochterski, P. Y. Ayala, K. Morokuma, G. A. Voth, P. Salvador, J. J. Dannenberg, V. G. Zakrzewski, S. Dapprich, A. D. Daniels, M. C. Strain, O. Farkas, D. K. Malick, A. D. Rabuck, K. Raghavachari, J. B. Foresman, J. V. Ortiz, Q. Cui, A. G. Baboul, S. Clifford, J. Cioslowski, B. B. Stefanov, G. Liu, A. Liashenko, P. Piskorz, I. Komaromi, R. L. Martin, D. J. Fox, T. Keith, M. A. Al-Laham, C. Y. Peng, A. Nanayakkara, M. Challacombe, P. M. W. Gill, B. Johnson, W. Chen, M. W. Wong, C. Gonzalez, J. A. Pople, Gaussian, Inc., Pittsburgh, PA, **2004**.
[27] A. D. Becke, *J. Chem. Phys.* **1993**, *98*, 5648.
[28] C. T. Lee, W. T. Yang, R. G. Parr, *Phys. Rev. B* **1988**, *37*, 785.
[29] P. J. Hay, W. R. Wadt, *J. Chem. Phys.* **1985**, *82*, 299.
[30] K. Fukui, *J. Phys. Chem.* **1970**, *74*, 4161.
[31] C. Gonzalez, H. B. Schlegel, *J. Phys. Chem.* **1990**, *94*, 5523.
[32] C. Gonzalez, H. B. Schlegel, *J. Chem. Phys.* **1991**, *95*, 5853.
[33] M. Cossi, G. Scalmani, N. Rega, V. Barone, *J. Chem. Phys.* **2002**, *117*, 43.
[34] J. Tomasi, B. Mennucci, R. Cammi, *Chem. Rev.* **2005**, *105*, 2999.
[35] D. Ardura, R. Lopez, T. L. Sordo, *J. Phys. Chem. B* **2005**, *109*, 23618.
[36] J. Cooper, T. Ziegler, *Inorg. Chem.* **2002**, *41*, 6614.
[37] B. O. Leung, D. L. Reidl, D. A. Armstrong, A. Rauk, *J. Phys. Chem. A* **2004**, *108*, 2720.
[38] F. P. Rotzinger, *Chem. Rev.* **2005**, *105*, 2003.
[39] S. Sakaki, T. Takayama, M. Sumimoto, M. Sugimoto, *J. Am. Chem. Soc.* **2004**, *126*, 3332.

Received: August 8, 2009
Published online: December 22, 2009

